JACS
JOURNAL OF THE AMERICAN CHEMICAL SOCIETY
Article
pubs.acs.org/JACS

Rotation Triggers Nucleotide-Independent Conformational Transition of the Empty β Subunit of F_1-ATPase

Jacek Czub[†] and Helmut Grubmüller[‡,*]

[†]Department of Physical Chemistry, Gdansk University of Technology, ul. Narutowicza 11/12, 80-233 Gdańsk, Poland
[‡]Department of Theoretical and Computational Biophysics, Max Planck Institute for Biophysical Chemistry, Am Fassberg 11, 37077 Göttingen, Germany

Supporting Information

ABSTRACT: F_1-ATPase (F_1) is the catalytic portion of ATP synthase, a rotary motor protein that couples proton gradients to ATP synthesis. Driven by a proton flux, the F_1 asymmetric γ subunit undergoes a stepwise rotation inside the $\alpha_3\beta_3$ headpiece and causes the β subunits' binding sites to cycle between states of different affinity for nucleotides. These concerted transitions drive the synthesis of ATP from ADP and phosphate. Here, we study the coupling between the mechanical progression of γ and the conformations of $\alpha_3\beta_3$. Using molecular dynamics simulations, we show that the nucleotide-free β subunit, initially in the open, low-affinity state, undergoes a spontaneous closing transition to the half-open state in response to the γ rotation in the synthesis direction. We estimate the kinetics of this spontaneous conformational change and analyze its mechanism and driving forces. By computing free energy profiles, we find that the isolated empty β subunit preferentially adopts the half-open conformation and that the transition to this conformation from the fully open state is accompanied by well-defined changes in the structure and interactions of the active site region. These results suggest that ADP binding to F_1 occurs via conformational selection and is preceded by the transition of the active site to the half-open conformation, driven by the intrinsic elasticity of β. Our results also indicate that opening of the nucleotide-free β during hydrolysis is not spontaneous, as previously assumed. Rather, the fully open conformation observed in the F_1 X-ray structure is enforced sterically by the γ subunit whose orientation is stabilized by interactions with the two other β subunits in the completely closed state. This finding supports the notion that γ acts by coupling the extreme conformational states of β subunits within the $\alpha_3\beta_3$ hexamer and therefore is responsible for high efficiency of the coordinated catalysis.

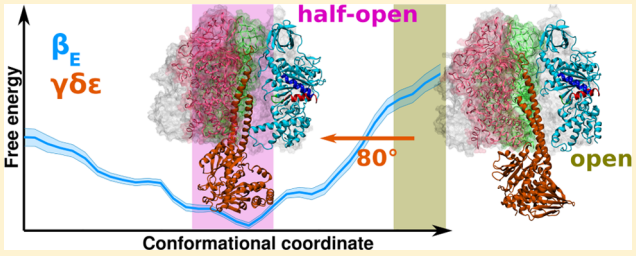

INTRODUCTION

F_oF_1-ATPase or ATP synthase is an important enzyme located in the inner mitochondrial membrane that uses the proton gradient across the membrane to synthesize ATP from ADP and inorganic phosphate.[1−3] When the proton gradient is low relative to the free energy of ATP hydrolysis, the protein may also operate in reverse direction, as an ATP-driven H^+-pump.[1−3]

ATP synthase consists of two mechanically coupled rotary motors, the membrane-embedded F_o that mediates proton translocation,[4−6] and the soluble F_1 (Figure 1A), responsible for ATP synthesis or hydrolysis.[1−3,7,8] In the mitochondrial form of the oligomeric F_1 motor, three subunits: γ, δ, and ε form the central asymmetric shaft (γ-shaft) surrounded by the catalytic head of hexagonally arranged α and β subunits (Figure 1A).[9,10] It is widely accepted that in synthesis mode, the proton-driven rotation of F_o induces a rotary motion of the γ-shaft (also referred to as the F_1 rotor) within the $\alpha_3\beta_3$ head (the F_1 stator).[2,3] For hydrolysis direction it was directly shown in single-molecule experiments that this rotation occurs in 120° steps, each associated with one catalytic cycle. The 120° steps of the γ-shaft were further resolved into 80° and 40° substeps,[11,12] which, in the hydrolysis direction, occur after the ATP-binding pause and the catalytic pause, respectively. The γ-shaft rotation causes the three active sites located at the β subunits to undergo cyclic conformational transitions between states of different nucleotide affinity (Figure 1A). These concerted conformational changes drive net synthesis of ATP against high cytosolic ATP:ADP concentration ratios.[1,2,9]

Despite extensive studies on the energy conversion mechanism in F_1-ATPase,[2,7,13−22] it is still not understood precisely how the sequential conformational changes within the catalytic head of the enzyme are mechanistically coupled to the rotation pattern of the γ-shaft. One intriguing aspect of this mechanism is the coupling between the angular position of the γ-shaft and the conformation of the nucleotide-free β subunit. In virtually all crystal structures of the F_1 complex the convex side of the γ-shaft is oriented toward the empty β subunit (β_E in Figure 1A) in its fully open conformation, usually associated with the low affinity state.[9,10] It is, however, not known if the γ-shaft forces β_E into this open, low-affinity state, by sterically

Received: January 6, 2014
Published: April 25, 2014

   dx.doi.org/10.1021/ja500120m | J. Am. Chem. Soc. 2014, 136, 6960−6968

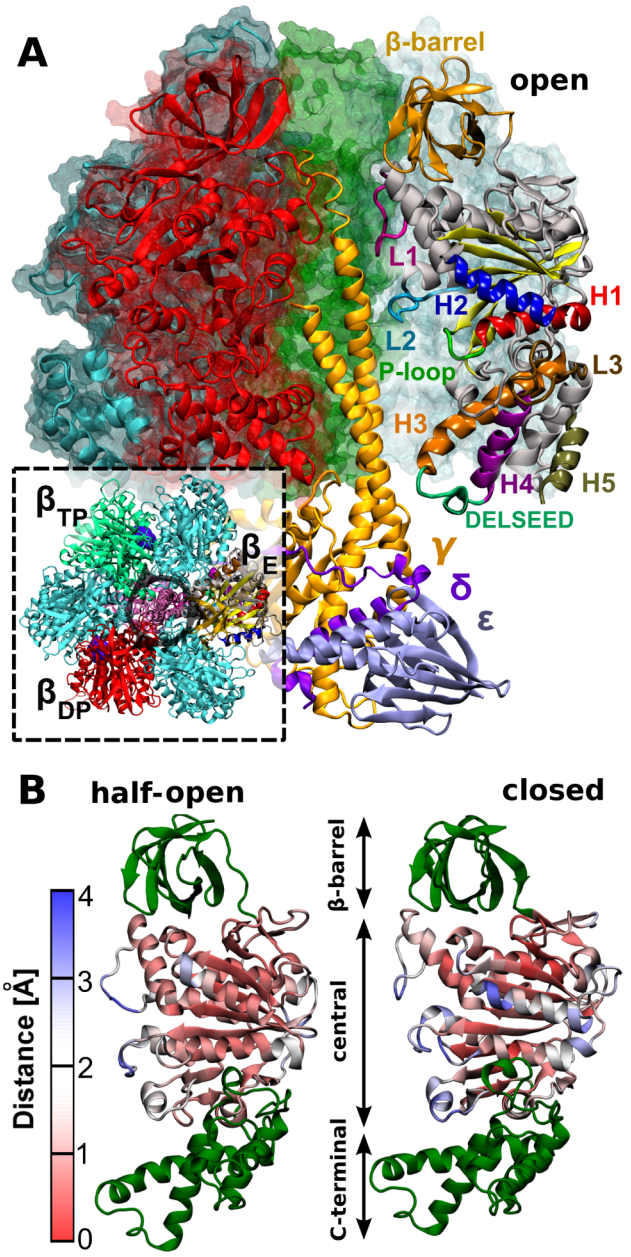

Figure 1. (A) Structure of F_1-ATPase showing the initial position of the γ-shaft ($\gamma\delta\varepsilon$ rotary subunit) at 0°. The nucleotide-free β subunit is initially in the open conformation and is used to define individual structural elements of the subunit. The two other β subunits are initially in the closed conformations and contain bound nucleotides. For clarity, one of the α subunits is not shown. Inset: topview of the F_1 structure showing the direction of rotation during ATP synthesis. β_{TP}, β_{DP}, and β_E denote the ATP-bound, ADP-bound and empty β subunits as defined in the original F_1 X-ray structure.[9] (B) Two other conformations of the nucleotide-free β: the half-open conformation (left) and closed conformation (right). To emphasize differences in the conformations of the binding site, the central domains are colored according to the residue-wise root-mean-square displacement (RMSD) between the open and half-open conformation (left) and between the half-open and closed conformation (right).

hindering the rotation of its lower half toward the central axis. Alternatively, the nucleotide-free β may adopt the open conformation spontaneously allowing the asymmetric γ subunit to be forced into the observed orientation, presumably by the interactions with the two remaining β subunits, β_{DP} and β_{TP}.

Elucidation of this problem is essential for understanding the coupling between the γ-shaft rotary motion and the conformational dynamics of the nucleotide-free β during the mechanochemical cycle. In particular, it would clarify the mechanism through which the F_o-induced rotation of the γ-shaft in the synthesis direction can cause β to switch between states differing in their affinity for nucleotides. Conversely, such insight would also reveal whether and how the intrinsic elasticity of the empty β is utilized in driving the γ-shaft rotation in the hydrolysis direction.

Recent experiments in which the stepped rotation is correlated with the crystal structure have shown that the original crystal structure of F_1 represents the catalytic dwell[23−25] and that the release of ADP in hydrolysis mode occurs in the ATP-binding dwell.[24,26−28] If this is the case, and if the process of energy transduction in F_1 is reversible as expected from its high efficiency,[29,30] then in the synthesis direction ADP binding should occur at +80° with respect to the crystal structure resting position of the γ-shaft. Therefore, understanding the intrinsic elasticity of the empty β would also allow clarifying if, in the ATP-dependent dwell, ADP binds to β_E before or after its transition to a higher affinity state, in other words, whether ADP binding to F_1 is governed by conformational selection or by induced fit.

Unfortunately, the data on the conformational behavior of the β subunits resulting from the previous studies are quite controversial. Initially, it was proposed that in the F_1 crystal structure resting state, the γ-shaft hinders the C-terminal domain of the β_E subunit, thereby preventing its transition from the open (low-affinity) state to the closed state.[9] This idea of a prestressed spring is consistent with the well-established finding that the release of a nucleotide molecule from the β-subunit requires energy input.[1,2] This notion, consistent with the conformational selection scenario, received further support from early molecular dynamics (MD) simulations of the complete F_1 complex.[31,32] Contrary to these predictions, subsequent NMR[33] and computational[34,35] studies, albeit of the isolated β subunit in solution, indicated that the nucleotide-free β subunit in solution assumes the conformation resembling the open state in F_1. According to these studies, the transition to the closed state requires nucleotide binding, consistent with the induced fit scenario. However, as seen from the crystallographic data, these conclusions might not apply to the F_1 complex in which nucleotide-depleted β subunits can still adopt the fully closed conformation.[36,37]

Here, we used all-atom MD simulations of the fully solvated complete F_1 complex, to study the relation between the angular position of the γ-shaft and the conformation of β_E, as well as the underlying energetics. To examine the conformational dynamics of β_E during a synthesis cycle, we simulated a complete 120° rotational step of F_1 using the flexible axis rotation approach.[38] We found that in response to the γ-shaft rotation, β_E, initially in the open state, undergoes fast spontaneous closure to a half-open conformation (Figure 1B). This finding shows that in the original crystal structure β_E is indeed arrested in the low-affinity state and that its transition toward higher-affinity state is not triggered by ADP or phosphate binding, but rather by the γ-shaft rotation. We also found that the half-open conformation is stable when the rotation of γ-shaft is stopped at +80°, a position that presumably corresponds to the ATP-binding dwell. Thus, we propose that the half-open conformation represents the intermediate state of β, recently revealed in the ATP-binding dwell.[24] Additionally, using free energy calculations and

dx.doi.org/10.1021/ja500120m | J. Am. Chem. Soc. 2014, 136, 6960−6968

interaction energy analysis, we identified electrostatic interactions between the α-helices forming the β binding site as one of the factors important for the observed spontaneous closure. Additional simulations predict that the transition is no longer spontaneous when all acidic residues of one of the helices are replaced by alanines, which also provides a straightforward experimental test of our above findings.

METHODS

Rotary Cycle Simulations. Initial coordinates of the protein were taken from the 2.4-Å crystal structure of the bovine F_1-ATPase (PDB code 1E79).[10] Two short missing loops in the γ subunit (62−66 and 97−100) were modeled with tCONCOORD.[39] The covalently bound inhibitor, glycerol, and sulfate molecules were removed, leaving the natural ligands Mg·ATP and Mg·ADP in their respective binding sites. The protein structure was solvated with 87 321 TIP4P water molecules[40] in a 16.7 × 13.8 × 13.8 nm rectangular box, at physiological ionic strength (140 mM NaCl). The OPLS/AA force field[41] was used for the protein, bound ligands, and ions.

All production MD simulations were run using Gromacs 4[42] in the NPT ensemble at 300 K and 1 bar using Nose−Hoover thermostat[43] and Parinello−Rahman barostat.[44] Periodic boundary conditions were applied in 3D, and electrostatic interactions were calculated using the particle mesh Ewald (PME) method[45] with a real-space cutoff of 1 nm and a Fourier grid spacing of 0.1 nm. A cutoff of 1 nm was used for Lennard−Jones interactions. Bond lengths were constrained using P-LINCS[46] for the protein and ligands and SETTLE[47] for water. The equations of motion were integrated using the leapfrog algorithm with a 2 fs time step.

Before inducing the rotor movement, the system was equilibrated as described in the paper by Kutzner et al.[38] and subjected to 500 ns of equilibrium MD. To sample conformational dynamics of F_1 during a single catalytic cycle, six independent enforced-rotation simulations were performed using initial conditions extracted from the last 50 ns of the obtained equilibrium ensemble. To mimic the effect exerted on F_1 by the rotating F_o motor, a flexible-axis method[38] that exerts a proper torque on all 272 C_α atoms of the γ subunit were chosen as rotation group. The longest principal axis of the $\alpha_3\beta_3$ stator was used as rotation vector. The rotor was driven in synthesis direction (Figure 1A), at an angular rate of 0.00042°/ps during 300 ns of simulation time with the spring constant of 600 kJ/(mol·nm^2).[38] This yielded a 120° rotation, which due to the F_1 symmetry covers a complete catalytic cycle. To mimic the immobilizing effect of the periphery stalk on the $\alpha_3\beta_3$ stator, all backbone atoms of six N-terminal residues of all β subunits were harmonically restrained to their initial positions.

To relax the system at a final position of the rotor and to characterize the conformation of β_E in the putative ATP-dependent dwell, additional MD simulations were performed in which the γ-shaft was kept at 120° and 80°, respectively. This was done with the same MD protocol as described above using snapshots from the enforced rotation simulations as the initial configurations. The γ subunit was restrained using the flexible-rotation method with angular velocity of 0 and spring constant of 600 kJ/(mol·nm^2).

As a test of our predictions, we performed the rotary cycle simulations for the F_1 mutant with all four acidic residues in the H2 helix (Figure 1) (Glu192, Asp195, Glu199, Glu202) replaced by alanines, using the same flexible-rotation protocol as for the wild type. The initial configurations for these simulations were taken from the last 50 ns of the 200 ns equilibrium simulation of the F_1 mutant, obtained by introducing alanines in the final snapshot of the 500 ns equilibrium simulation of the wild type.

Free Energy along the Conformational Coordinate. As a collective coordinate describing the open-to-closed conformational transition of the β subunit we used the projection on the first eigenvector of the Cα covariance matrix computed from the combined trajectories of β_E and β_{TP} extracted from the 500 ns equilibrium ensemble of the F_1-ATPase. This eigenvector is approximately parallel to the vector joining the closed and open crystal structure conformations (cyan circle and green square, respectively, in Figure 2A). The free energy profile along this coordinate for the isolated nucleotide-free β subunit was calculated using umbrella sampling.[48] A total of 30 umbrella windows were used, spaced 0.5 nm apart and spanning the range from −7 nm (closed state) to 7 nm (open state). Initial protein configurations for these windows were extracted from a single induced-rotation run (blue in Figure 2B). All protein structures

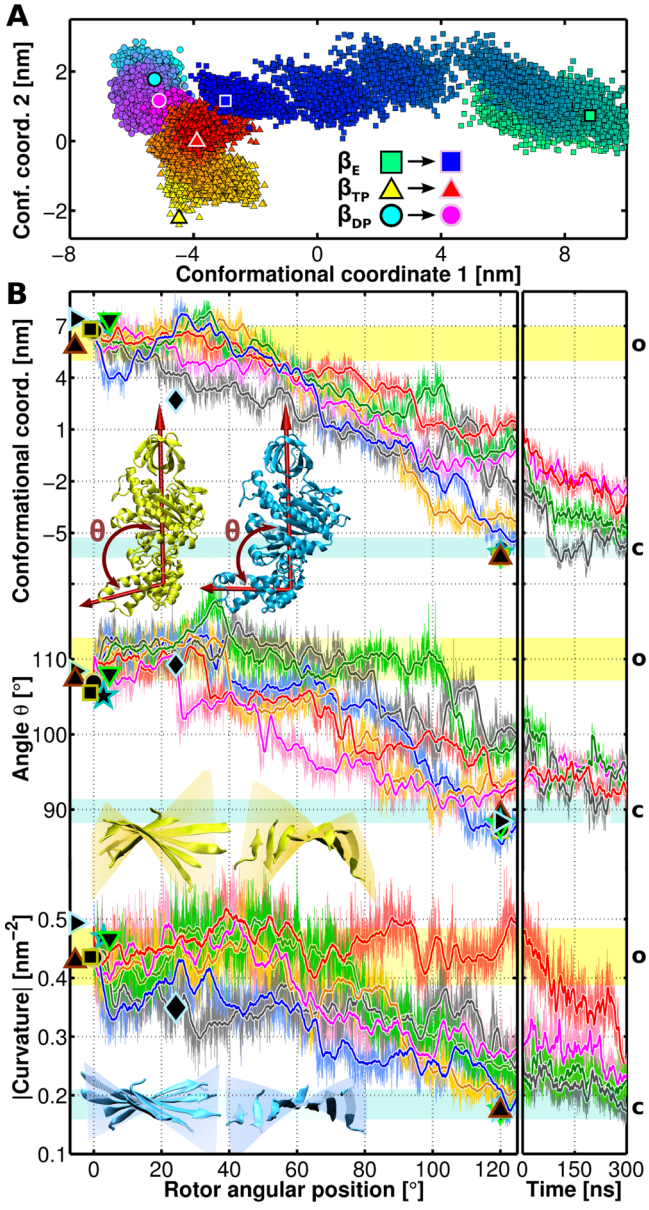

Figure 2. (A) The projection of the three β trajectories from a single flexible-rotation run on the plane defined by their initial X-ray structures. (B) Conformational dynamics of the empty β subunit during six independent, 300 ns flexible-rotation cycles of F_1 (0 → 120°): the overall conformational coordinate (top), the bend angle θ (middle), and the curvature of the central domain β-sheet (bottom) as a function of the γ-shaft angular position. Yellow and blue shaded areas show the extent of fluctuations of the analyzed parameters at the initial resting state (0°) for the open and closed conformation, respectively. The panel on the right show changes of the further evolution of the parameters during the additional 300 ns run with the γ-shaft kept at its final position (120°). The markers show values of the analyzed parameters for the open (0°), half-closed (24°), and closed (120°) conformations taken from several F_1 X-ray structures (◆ 1H8E; ★ 1BMF; ▼ 2JIZ; ■ 2WSS; ● 1E79; ▶ 2HLD; ▲ 2 V7Q).

dx.doi.org/10.1021/ja500120m | J. Am. Chem. Soc. 2014, 136, 6960−6968

were solvated with a 140 mM NaCl aqueous solution in a rhombic dodecahedron box with a minimum distance of 1.5 nm between the protein and the box boundary. The systems were simulated for 250 ns using the same protocol as described above. During first 10 ns all backbone atoms were harmonically restrained to their initial positions. The harmonic potential with a force constant of 100 kJ/(mol·nm^2) was used as the umbrella potential along the conformational coordinate. Free energy profiles were determined from the last 200 ns of production simulations using the standard weighted histogram analysis method (WHAM).[49] Error bars were estimated using Monte Carlo bootstrap analysis.

Data Analysis. The main bend angle of the β subunit was defined as the angle between the longest principal axes of the β-barrel/central domain (residues Thr9−Ile357) and the C-terminal domain (residues Met358−Glu475).

To determine the curvature of the β-sheet in the central domain, a second-order surface $s(u, v)$ was first fitted to the positions of all C_α atoms of the residues forming the β-sheet. Subsequently, principal curvatures, κ_1 and κ_2, of the obtained surface $s(u, v)$ were determined as the eigenvalues of the Hessian of $s(u, v)$ and multiplied to get the Gaussian curvature of the β-sheet, $G = \kappa_1\kappa_2$.

To calculate the populations of different types of secondary structures along the β chain, we first assigned secondary structures to all β conformations obtained from the umbrella sampling (US) simulations using DSSP algorithm.[50] Subsequently, the equilibrium secondary structure populations were computed for each residue of β by weighting the biased distributions by a factor of $\exp[(V_i(\xi) - F_i)/k_BT]$, where $V_i(\xi)$ and F_i denote the biasing potential and the WHAM free energy constant, respectively, corresponding to the i-th US window.

All molecular images were created using VMD.[51]

RESULTS AND DISCUSSION

Conformational Transition of β_E during the Rotary Cycle. To examine the conformational behavior of the β_E subunit during the 120° rotation cycle of F_1-ATPase, we performed six independent all-atom MD simulations of the F_1 holoenzyme, in which the γ-shaft (Figure 1A) was driven to rotate for 300 ns, in the synthesis direction. This 120° rotation was followed by 300 ns simulation in which the γ-shaft was kept in place to allow for structural relaxation. The performed simulated rotations were by 2 orders of magnitude slower than in our previous study[52] and thus allowed us to better characterize the conformational response of the $\alpha_3\beta_3$ stator to the γ-shaft motion. It should be mentioned, however, that even the current simulations do not allow capturing all slow relaxation processes (1 μs−1 ms) that might be important for the coordinated rotary catalysis. Because of a relatively high angular velocity, the average external torque applied to the γ subunit in our simulations was equal to ∼600 pN·nm, which is 1 order of magnitude larger than the torque estimated for the active F_1 motor in hydrolysis mode (∼40−50 pN·nm).[7,13]

During the simulated rotary step, the convex surface of the coiled-coil γ subunit rotates within the $\alpha_3\beta_3$ stator, from its initial angular position (0°), at which it points toward the β_E subunit (empty), to the final position (+120°), at which it points toward the β_{TP} subunit (nucleotide-bound). For all these flexible-axis rotations,[38] marked conformational changes of the β_E subunit were observed as a result of the rotor motion (Figure 1B). To quantify the extent of these conformational changes, the trajectories of all three β subunits were first projected onto the conformational hyperplane defined by their X-ray structures: β_E, β_{TP}, and β_{DP}[10] (Figure 2A). As can be seen, in response to the γ-shaft rotary progression, the open β subunit spontaneously moves toward its closed state within 300 ns. This result suggests that this closing motion in not only nucleotide-independent, but also unexpectedly fast.

Figure 2B relates the β_E conformational coordinate (see Methods) to the γ-shaft angular position for our six simulations. As can be seen in all simulations, following the γ-shaft progression, β_E underwent a transition from the initial open conformation (∼6 nm) toward the closed conformation (∼−6.5 nm). In two cases, the transition of β_E from the open to the closed state is fully completed already after 300 ns of the actual flexible-axis rotation. When we continued the simulations while keeping the rotor at its final position, almost full closure of β_E was observed for the other four runs as well (Figure 2B). The finding that the β subunit can adopt a close conformation in the F_1 complex without binding a nucleotide is consistent with the crystallographic data.[37]

To gain more detailed structural insight into the observed β_E conformational changes, we determined how the curvature of the β-sheet in the central domain and the bend angle θ between the β-barrel/central and the C-terminal domains (Figure 2B insets) change with the γ-shaft angular position. It can be seen in Figure 2B that the rotation of the γ-shaft is accompanied by flattening of the β-sheet from the curvature of ∼0.45 to ∼0.25 nm^{-2} and by a ∼20° decrease of the angle θ leading to a more compact structure of the subunit. These structural changes of β_E are fully consistent with the open−closed transition as inferred from the X-ray data.[9,10] As a result of the observed transition, the fluctuations of the β-sheet curvature and the angle θ, shown in Figure 2B, are also reduced by about 50%, which reflects differences in the equilibrium dynamics of the open and closed states inferred from MD simulations.[53]

Figure 2B also shows that the conformation of β_E is highly correlated with the angular position of the γ-shaft, suggesting a tight coupling between the angular progression of the rotor and the conformational state of the catalytic part of F_1-ATPase. This finding is consistent with the crystallographic data[54] showing that when the γ-shaft is moved by 20° in the synthesis direction from its typically observed orientation, β_E adopts an intermediate conformation (β_{HC}, ∼2.8 nm, see diamond symbol in Figure 2B) that is actually very similar to the one predicted by our simulations.

The conformational state of β_E can be seen in Figure 2B to closely follow the rotation of the γ-shaft even in our simulations, which are presumably faster by up to a factor of 100[2,3] than the rotation speed of the γ subunit under physiological conditions. This result suggests that under physiological conditions, the conformational transition of β, progressing under the presence of γ, is about 1 to 2 orders of magnitude faster than ADP binding, which occurs on the 0.1−1 ms time scale.[55] Accordingly, the ADP binding in the synthesis direction should be preceded by the transition of β_E to a state characterized by higher affinity for nucleotides.

This finding is consistent with single-molecule imaging data showing that the release of ADP during hydrolysis occurs in the so-called ATP-dependent dwell in which the γ-shaft is rotated by 80° from the position observed in the crystal structure.[27] Our simulations also predict that in the ATP-dependent dwell β_E is in the intermediate conformation, and therefore ADP binding is governed by conformational selection. Note that in additional simulations (Figure S1, Supporting Information) the intermediate conformation is stable over 400 ns when the γ-shaft is kept at +80°. This finding may provide a structural interpretation for single-molecule data suggesting that in ATP-

dependent dwell β_E adopts a state that is structurally distinct from the usually observed open and closed conformations.[24]

Conformational Equilibrium of the Empty β Subunit. We next asked what is the underlying molecular mechanism for the observed conformational changes of β_E during the catalytic cycle and, in particular, what is the mechanism stabilizing the intermediate conformation of β_E that is, as proposed here, adopted in the ATP-dependent dwell. To answer these questions, we first computed the free energy profile governing the conformational equilibrium of the isolated empty β subunit. To this end we applied umbrella sampling (US) for a set of initial configurations of β_E spanning the open−closed transition observed in our simulations of the F_1-ATPase rotary cycle (see Methods for details).

Figure 3A shows that the free energy of the isolated, nucleotide-free β subunit exhibits a clear minimum in the middle region of the conformational pathway (~0−2 nm) in between the open and closed states. Therefore, already for the isolated β, the intermediate conformation is by 2.3 and 2.0 kcal/mol, respectively, more favorable than the two extreme states and does not require external stabilization by the F_1 complex constituents. As demonstrated by the RMSD profiles from the three distinct X-ray conformations (Figure 3B), the preferred conformation is most similar, in terms of the central domain structure, to the half-closed state β_{HC} and, to a lesser extent, to the open state. Thus, it will be referred to as the half-open conformation, β_{HO}.

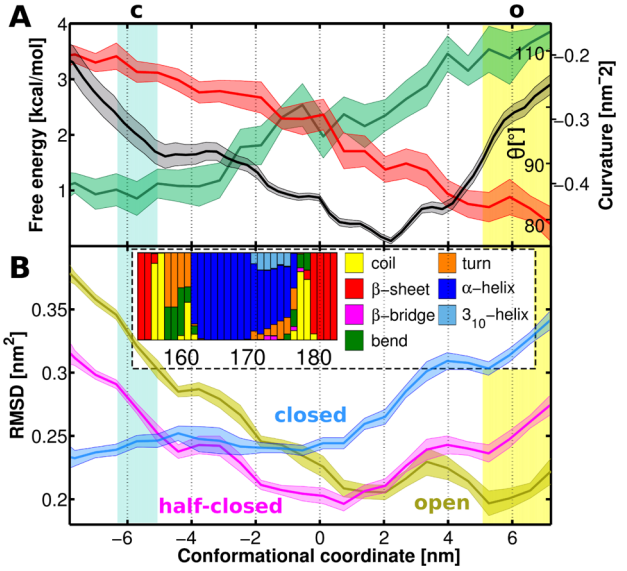

Figure 3. (A) The free energy profile for the open-to-closed transition of the isolated nucleotide-free β subunit (black). Changes of the average bending angle θ (green) and the average curvature of the central domain β-sheet (red) along the conformational coordinate show that the studied equilibrium captures main features of the open-to-closed transition in the F_1 complex (for full distributions of these and other parameters characterizing the structure of β along the conformational coordinate see Figure S2, Supporting Information). (B) Similarity of the isolated β sampled along the conformational pathway to the three F_1 crystal structure conformations, expressed as the central domain RMSD. Inset: Equilibrium populations of different secondary structure for residues 154−183 (H1 region) of the isolated nucleotide-free β (for all residues, see Figure S3, Supporting Information).

The residue-based RMSD coloring of the central domain (Figure 1B) reveals that main differences between the half-open conformation and both the open and the closed conformation are located near the binding site (the P-loop and the helices H1 and H2) and at the surface that in F_1 contacts with the rotor (loops L1 and L2). Upon transition from the open (low-affinity) state to the half-open state, the relative arrangement of the helices H1 and H2 progresses toward the orientation found in the closed (high-affinity) state (see Figure 1B and Figure S2, Supporting Information). This intermediate structure of the binding site in the half-open conformation is expected to increase the affinity of β for nucleotide as evidenced by the crystal structure in which the β_{HC} subunit with a similar conformation of the binding site is filled with ADP and Pi.[54] Therefore, the half-open empty β is likely to provide the medium affinity binding site, which in the synthesis mode binds ADP in the ATP-dependent dwell (+80°), in agreement with single-molecule experiments.[24]

On the basis of NMR measurements, it has been suggested that in the absence of ADP or ATP, the isolated β subunit adopts the open conformation,[33] which seems to disagree with our above findings. To resolve this issue, we tested whether or not the NMR structural data are also compatible with the half-open conformation that was previously not considered. To that aim, we examined two structural parameters studied by Yagi et al.[33] First, we determined, by properly reweighting the US trajectory data, the equilibrium populations of different types of secondary structures along the β chain (Figure S3, Supporting Information) and compared them with the average secondary structure assigned on the basis of chemical shifts.[33] The inset in Figure 3 shows that in equilibrium, dominated by the half-open conformation, the C-terminal part of the H1 region (residues 171−175) is α-helical, as it is in the open conformation. The second structural parameter considered by Yagi et al.[33] was the angle describing the relative orientation of the N-terminal domain (residues 1−124; β-barrel and the top of the central domain) and the C-terminal domain (residues 391−473; helices H4 and H5 and loop L3). We found that the average value of this angle determined using $^1H-^{15}N$ residual dipolar couplings (144°) is similar to its equilibrium ensemble average of 138 ± 3° obtained from our data (see Figure S2D, Supporting Information). We therefore consider the NMR data compatible with the conformational selection scenario suggested by our simulations. In particular, although the two above parameters allow one to study the relative populations of the open and closed conformations, they cannot be directly used to discriminate between the former and the half-open state, mainly because these conformations are quite similar.

This finding also suggests several possible experimental tests. Comparison of Figure S2B,D (Supporting Information) suggests, e.g., that one might include the H3 helix into the spin-labeled segment defining the bending angle. This helix largely specifies the orientation of the C-terminal domain and causes the bending angle to be almost linearly dependent on the overall conformational coordinate. Alternatively, the distance between the N-terminal region of helix H1 and C-terminal region of helix H2 might also serve as a parameter allowing for studying equilibrium between all the three conformational states of β.

The RMSD to the crystal structure β_{DP} shown in Figure 3B indicates that the closed conformation reached during the rotation in the absence of a nucleotide differs markedly from the crystallographic one. Although the empty β can be forced

dx.doi.org/10.1021/ja500120m | J. Am. Chem. Soc. 2014, 136, 6960−6968

by rotating γ-shaft to bend up to the θ angles characteristic for the β_{DP} or β_{TP} (see discussion below), this change does not propagate fully toward the central domain and, in particular, to the binding site. This observation indicates that in the absence of a nucleotide, a transition of the empty β to the actual β_{DP} or β_{TP} is highly unfavorable, in agreement with the free energy calculations showing that in this case the β_{TP} state is destabilized by 6.0 kcal/mol relative to the open state.[34]

Mechanism and Molecular Driving Forces of the β_E Conformational Change. The profile in Figure 3A also shows that the free energy energy of the half-open conformation is lower than that of the open state, thus providing further and independent evidence for spontaneous closure of the β_E subunit after the γ-shaft has rotated away from the initial angular position (0°). At 0°, the convex side of γ imposes a steric hindrance against the empty β subunit and stabilizes it in the fully open, low-affinity conformation. This stabilization is achieved through strong interaction between the globular portion of γ and the DELSEED regions of the C-terminal domains of β_{TP} and β_{DP}, which as we have recently shown[53] is responsible for stabilizing the angular position of the γ-shaft around 0°. Indeed, as shown in Figure S4 (Supporting Information), the rotation from the 0° dwell position requires breaking the interactions between γ and C-terminal domains of the two β subunits in the closed state (β_{TP} and β_{DP}), which gives rise to the large activation barrier for this rotary substep. This finding suggests that at 0° γ couples opening of one β subunit to nucleotide-induced closing of the two other and therefore supports the role of γ as an element responsible for efficient and precise coordination of the functional states within the $\alpha_3\beta_3$ hexamer.

To examine the energetics that governs the spontaneous transition toward the half-open conformation, in Figure 4A we plotted the intraprotein enthalpic contribution to the interaction free energy along the conformational coordinate. In Figure 4B, this contribution is additionally decomposed into interactions between individual structural elements of the β subunit. As can be seen, there are only several interactions that vary markedly (>30 kcal/mol) along the closing pathway and thus are thought to contribute significantly to the shape of the overall free energy profile. Note, however, that all these contributions are dominated by electrostatic interactions and are typically strongly compensated by other factors not included in this analysis, in particular, by solvation energies, as seen from Figure 4A, and possibly by conformational and solvation entropies. Although very often interaction free energies correlate with the underlying enthalpies,[56] our analysis of intraprotein interaction enthalpies can only capture part of the driving forces of the closing mechanism.

Figure 4B indicates that the intraprotein closing energy is dominated by the interactions between the elements forming the hinge region of β_E, especially the binding site. In particular, the initial closure of β (7 → 0 nm) is accompanied by the pronounced strengthening of interactions between helices H1 and H2, with the optimal interaction energy between them found around 0 nm. The interaction between H2 and the flexible loop L3 and intra-β-sheet interactions are also enhanced upon this transition. It can be further seen that the apparent breakdown of the intraprotein interaction in the region 0−4 nm (Figure 4A) is mostly due to the loss of contacts between L3 and helix H5 located in the C-terminal-domain (Figure 4B, bottom). The hydration energy of L3 and, to a lesser extent, of H5 compensates for this loss and may be responsible for

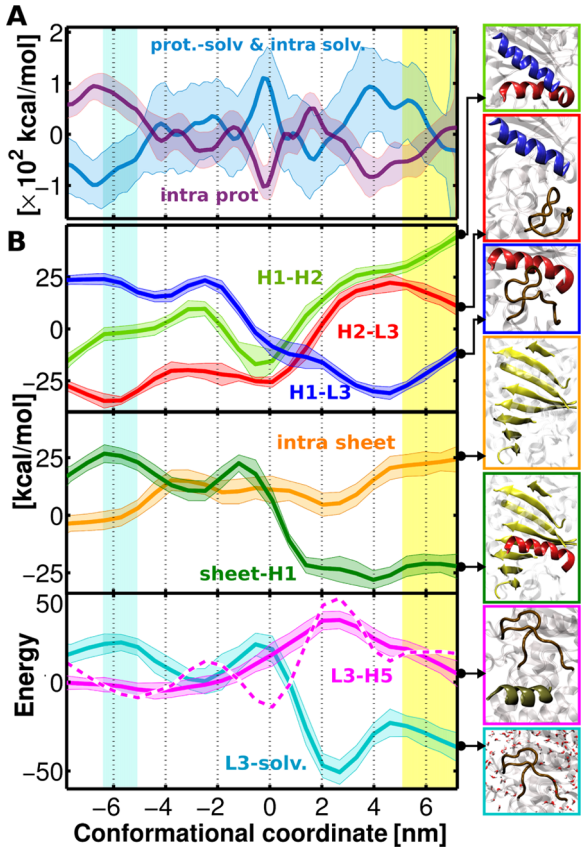

Figure 4. (A) Main contributions to interaction free energy along the open-to-close transition for the isolated β. (B) Decomposition of the intraprotein part into individual contributions. Only the interactions contributing more than 30 kcal/mol to the intraprotein energy change are presented. Definitions of the structural elements is consistent with Figure 1. The dashed-pink curve shows the interaction between the L3 loop and the rest of the protein structure.

shifting the minimum of the half-open conformation from 0 nm, preferred for strongest H1−H2 interaction, to 2 nm.

Put together, the above analysis suggests the following mechanism of the initial spontaneous closure of β_E. In its initial position, the γ-shaft deforms the empty β by pressing on its C-terminal domain (to the right and downward in Figure 1). The resulting strain propagates from helix H3, through electrostatic and hydrophobic contacts (K382−D349, R372−D359−R357 and L378−L351, V374−L143−P350, respectively) to the lower part of the β-sheet and further, via a short P-loop and the charge pairs D256−K162 and D250−H177 from the β-sheet to helix H1 (Figure S5, Supporting Information). As a result, in a fully open conformation, H1 is displaced by about 0.5 nm to the right from its energetically optimal position relative to H2 (Figure S6, Supporting Information). Upon γ rotation, the C-terminal domain is released allowing the binding site to relax through shifting H1 to the left relative to H2 with only a slight change in the angular orientation between the helices (see angles ψ and σ in Figure S2, Supporting Information). Consequently, the P-loop moves away from the negatively charged bottom surface of H2, which should be expected to increase the affinity for nucleotides and phosphate (Figure S6, Supporting Information). At the same time, the lower portion of β, attached rigidly to H1, also protrudes toward the center of the stator. The resulting half-open conformation is stabilized by the formation of salt bridges K175−E202 and K162−E192 and

dx.doi.org/10.1021/ja500120m | J. Am. Chem. Soc. 2014, 136, 6960−6968

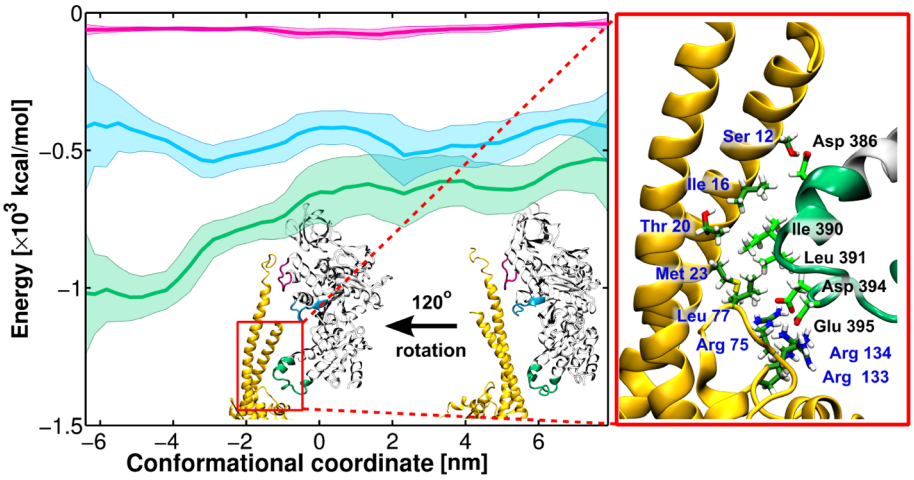

Figure 5. Interaction energy between the γ-shaft and the empty β and as a function of the conformational state of the latter during the simulated rotary cycle of F_1. Data is averaged over all independent flexible-rotation runs. Inset shows the favorable contact between β and γ after a complete 120° rotary cycle.

a hydrogen bond N171−S203 between H1 and H2 (Figure S6, Supporting Information). Flattening of the β-sheet and a decrease of the electrostatic repulsion between H2 and the flexible loop L3 provide additional stabilization.

Our above free energy and interaction profiles also show that, in the absence of a nucleotide molecule, the further transition of the isolated β from the half-open state to a completely closed state (0→ −6 nm) leads to the disruption of interactions within the protein, in particular, between H1 and the β-sheet (Figure 1B top) (D256 switches from K162 to T163, H177−D250 interaction weakens, Figure S6, Supporting Information) and to the increased repulsion between H1 and L3 (Figure 1B middle). This destabilizing effect may, therefore, be a factor preventing the isolated subunit from complete closure, in agreement with the free energy profile shown in Figure 3A.

What, then, drives the subsequent full closure of β_E during the rotary cycle of F_1 as evident from Figure 2? To address this question, we examined the interactions between the constituents of the full F_1 complex. We found that the closure of β is strongly correlated with strengthening of interactions between its C-terminal domain and the rotating γ subunit (Figure 5A). To form salt bridges and hydrophobic contacts with the approaching globular domain of γ (Figure 5B), the β C-terminal domain gradually moves up causing the entire lower portion of the subunit to rotate upward by about 20°. As a result, the closed conformation can be adopted with H1 oriented almost parallel to H2 (Figure S2EF, Supporting Information) and the P-loop moved away form the negatively charged surface of H2 (Figure S6, Supporting Information). This finding suggests that the closed conformation of the nucleotide-free β, as observed both in crystal structures[36,37] as well as in our simulations, is mainly stabilized by interactions with the γ globular domain and that this interaction may be necessary for the β subunit to adopt a completely closed conformation.

Effect of Mutations in the Binding Site on the Conformational Behavior of β_E. To further test if interactions between helices H1 and H2 are indeed important for the closure of the empty β, we replaced four negatively charged residues of the β_E H2 helix (Glu192, Asp195, Glu199, Glu202; Figure S6, Supporting Information) with alanines, such that the stabilizing H1−H2 contacts cannot be formed. We then repeated the flexible-axis rotation of the γ-shaft for the this F_1 mutant, as described above. Indeed, as can be seen from Figure 6, no transition to the half-open state upon γ rotation is

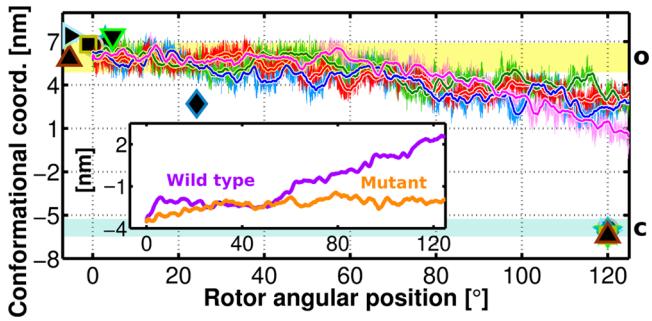

Figure 6. Conformational dynamics of the β_E mutant (all acidic residues in H2 replaced by Ala) during four independent 300 ns flexible-rotation cycles of F_1. To emphasize differences in the behavior of the wild-type and mutant, definition of the conformational coordinate in the inset is restricted to the binding site. See also Figure S7 (Supporting Information).

seen, in contrast to the wild type. Instead, starting from the intermediate position of the γ-shaft, β_E proceeds much slower along the conformational coordinate but does not reach the fully expressed half-open state. This limited closure is caused by gradual enhancement of interactions between the C-terminal domain of β_E and the globular domain of the rotating γ and leads to only partial bending of the subunit and less pronounced flattening of the β-sheet (Figure S7, Supporting Information). The effect exerted on the conformation of the binding site is even less evident, as shown in the inset of Figure 6. These results underscore the importance of the H1−H2 interactions for the spontaneous transition to the half-open state and also suggests an experimental test of our predictions. It should be noted, however, that other factors may also play a role in driving the closing transition, especially as electrostatically induced association of H1 and H2 is compensated by unfavorable dehydration energy and may be accompanied by packing changes in the F_1 complex. Indeed, it has been recently proposed that the solvent entropy changes originating from

dx.doi.org/10.1021/ja500120m | J. Am. Chem. Soc. 2014, 136, 6960−6968

packing rearrangements in F_1 may be crucial for driving the γ-shaft rotation in hydrolysis direction.[19,57,58]

CONCLUSIONS

In this work, we show that a nucleotide-free β subunit, initially in the open state (β_E), undergoes a fast closing transition in response to the rotation of the γ-shaft, induced in the fully atomic model of F_1-ATPase. The half-open state (β_{HO}) of the empty β reached after 80° rotation in the synthesis direction is stable when the γ-shaft is kept at this angular position, and likely corresponds to the so-called ATP-binding dwell.[23−25] The conformational free energy profile that we obtained for the isolated empty β suggests that the observed transition to the half-open state is spontaneous, i.e., it is driven by the intrinsic elasticity of the β subunit. Further closing of the isolated β beyond the half-open state is energetically disfavored. However, full closure is enforced in F_1-ATPase by strong and transient interactions with the rotating γ-shaft, as revealed by our flexible-rotation simulations. Closer analysis of the intrasubunit enthalpic contributions to the obtained free energy profile indicates that the conformational behavior of β_E is determined, at least to some extent, by electrostatic interactions between the helices H1 and H2 forming the active site as well as between these two and their surroundings. This finding is supported by the observation that the preference for β_{HO} can be strongly reduced by replacing acidic residues of H2 with alanines.

Our results also support the single-molecule rotation data showing that the X-ray structure (at 0°) most likely represents the catalytic dwell.[23−25] Our simulations further suggest that ADP binding at +80° is preceded by the spontaneous and fast transition of the empty β to the half-open state, which is characterized by a higher affinity for a nucleotide ligand, implying a conformational selection mechanism for ADP binding to F_1.

Moreover, the elastic behavior of the empty β characterized by our simulations shows that during the hydrolysis cycle the γ-shaft is not likely to be be pulled into the angular position observed in the X-ray structure by spontaneous opening of the nucleotide-free β, as it has been previously proposed (a "push−pull mechanism").[2,14] Conversely, full opening of the empty β is enforced sterically by the γ-shaft. According to our simulations, the energy required for this opening is provided by optimizing favorable electrostatic interactions between the globular portion of γ and the C-terminal domains of β_{TP} and β_{DP}. Our results further imply that that in hydrolysis mode the elastic free energy stored in the empty β subunit might be utilized in driving the 40° substep of F_1 from the catalytic dwell (X-ray structure) to the ATP-dependent dwell.

It has recently been found using atomic force microscopy that even without γ subunit the $\alpha_3\beta_3$ complex may still propagate unidirectionally in the presence of ATP, although much slower and in a less precise manner compared to the complete F_1 motor.[20] This propagation was proposed to be driven by water entropy changes through the so-called "packing exchange mechanism".[58] Our current data suggest that limited efficiency of such rotorless calalysis might result from the lack of tight coordination between states of different affinities for nucleotides provided by the γ subunit. In particular, our simulations indicate that without the stabilization imposed by γ, the β subunit cannot adopt a fully open low-affinity functional state.

ASSOCIATED CONTENT

Supporting Information

Detailed characterization of the β subunit conformational equilibrium. This material is available free of charge via the Internet at http://pubs.acs.org.

AUTHOR INFORMATION

Corresponding Author

hgrubmu@gwdg.de

Notes

The authors declare no competing financial interest.

ACKNOWLEDGMENTS

This work was supported by the EU Nanomot (NEST 029084) and ESF Eurocores Nanocell projects and by the Polish Ministry of Science and Higher Education (Project No. IP2012 03472).

REFERENCES

(1) Boyer, P. *Annu. Rev. Biochem.* **1997**, *66*, 717−749.
(2) Kinosita, K., Jr.; Adachi, K.; Itoh, H. *Annu. Rev. Biophys. Biomol. Struct.* **2004**, *33*, 245−268.
(3) Junge, W.; Sielaff, H.; Engelbrecht, S. *Nature* **2009**, *459*, 364−370.
(4) Stahlberg, H.; Müller, D.; Suda, K.; Fotiadis, D.; Engel, A.; Meier, T.; Matthey, U.; Dimroth, P. *EMBO Rep.* **2001**, *2*, 229−233.
(5) Düser, M.; Zarrabi, N.; Cipriano, D.; Ernst, S.; Glick, G.; Dunn, S.; Börsch, M. *EMBO J.* **2009**, *28*, 2689−2696.
(6) Pogoryelov, D.; Klyszejko, A. L.; Krasnoselska, G. O.; Heller, E.-M.; Leone, V.; Langer, J. D.; Vonck, J.; Müller, D. J.; Faraldo-Gómez, J. D.; Meier, T. *Proc. Natl. Acad. Sci. U. S. A.* **2012**, *109*, E1599−E1608.
(7) Noji, H.; Yasuda, R.; Yoshida, M.; Kinosita, K. *Nature* **1997**, *386*, 299−302.
(8) Sabbert, D.; Engelbrecht, S.; Junge, W. *Proc. Natl. Acad. Sci. U. S. A.* **1997**, *94*, 4401−4405.
(9) Abrahams, J.; Leslie, A.; Lutter, R.; Walker, J. *Nature* **1994**, *370*, 621−628.
(10) Gibbons, C.; Montgomery, M.; Leslie, A.; Walker, J. *Nat. Struct. Mol. Biol.* **2000**, *7*, 1055−1061.
(11) Yasuda, R.; Noji, H.; Yoshida, M.; Kinosita, K.; Itoh, H. *Nature* **2001**, *410*, 898−904.
(12) Shimabukuro, K.; Yasuda, R.; Muneyuki, E.; Hara, K. Y.; Kinosita, K.; Yoshida, M. *Proc. Natl. Acad. Sci. U. S. A.* **2003**, *100*, 14731−14736.
(13) Yasuda, R.; Noji, H.; Kinosita, K.; Yoshida, M. *Cell* **1998**, *93*, 1117−1124.
(14) Wang, H.; Oster, G. *Nature* **1998**, *396*, 279−282.
(15) Gao, Y.; Yang, W.; Karplus, M. *Cell* **2005**, *123*, 195−205.
(16) Xing, J.; Liao, J.; Oster, G. *Proc. Natl. Acad. Sci. U. S. A.* **2005**, *102*, 16539.
(17) Sielaff, H.; Rennekamp, H.; Wächter, A.; Xie, H.; Hilbers, F.; Feldbauer, K.; Dunn, S.; Engelbrecht, S.; Junge, W. *Proc. Natl. Acad. Sci. U. S. A.* **2008**, *105*, 17760.
(18) Mukherjee, S.; Warshel, A. *Proc. Natl. Acad. Sci. U. S. A.* **2011**, *108*, 20550−20555.
(19) Yoshidome, T.; Ito, Y.; Ikeguchi, M.; Kinoshita, M. *J. Am. Chem. Soc.* **2011**, *133*, 4030−4039.
(20) Uchihashi, T.; Iino, R.; Ando, T.; Noji, H. *Science* **2011**, *333*, 755−758.
(21) Beke-Somfai, T.; Lincoln, P.; Nordén, B. *Proc. Natl. Acad. Sci. U. S. A.* **2013**, *110*, 2117−2122.
(22) Okazaki, K.; Hummer, G. *Proc. Natl. Acad. Sci. U. S. A.* **2013**, *110*, 16468−16473.
(23) Okuno, D.; Fujisawa, R.; Iino, R.; Hirono-Hara, Y.; Imamura, H.; Noji, H. *Proc. Natl. Acad. Sci. U. S. A.* **2008**, *105*, 20722−20727.

(24) Masaike, T.; Koyama-Horibe, F.; Oiwa, K.; Yoshida, M.; Nishizaka, T. *Nat. Struct. Mol. Biol.* **2008**, *15*, 1326−1333.
(25) Sielaff, H.; Rennekamp, H.; Engelbrecht, S.; Junge, W. *Biophys. J.* **2008**, *95*, 4979−4987.
(26) Adachi, K.; Oiwa, K.; Nishizaka, T.; Furuike, S.; Noji, H.; Itoh, H.; Yoshida, M.; Kinosita, K. *Cell* **2007**, *130*, 309−321.
(27) Watanabe, R.; Iino, R.; Shimabukuro, K.; Yoshida, M.; Noji, H. *EMBO Rep.* **2008**, *9*, 84−90.
(28) Watanabe, R.; Iino, R.; Noji, H. *Nat. Chem. Biol.* **2010**, *6*, 814−820.
(29) Kinosita, K.; Yasuda, R.; Noji, H.; Adachi, K. *Philos. Trans. R. Soc., B* **2000**, *355*, 473−489.
(30) Pänke, O.; Cherepanov, D.; Gumbiowski, K.; Engelbrecht, S.; Junge, W. *Biophys. J.* **2001**, *81*, 1220−1233.
(31) Böckmann, R. A.; Grubmüller, H. *Nat. Struct. Biol.* **2002**, *9*, 198−202.
(32) Böckmann, R. A.; Grubmüller, H. *Biophys. J.* **2003**, *85*, 1482−1491.
(33) Yagi, H.; Tsujimoto, T.; Yamazaki, T.; Yoshida, M.; Akutsu, H. *J. Am. Chem. Soc.* **2004**, *126*, 16632−16638.
(34) Ito, Y.; Oroguchi, T.; Ikeguchi, M. *J. Am. Chem. Soc.* **2011**, *133*, 3372−3380.
(35) Kleinekathöfer, U.; Isralewitz, B.; Dittrich, M.; Schulten, K. *J. Phys. Chem. A* **2011**, *115*, 7267−7274.
(36) Groth, G.; Pohl, E. *J. Biol. Chem.* **2001**, *276*, 1345−1352.
(37) Kabaleeswaran, V.; Shen, H.; Symersky, J.; Walker, J.; Leslie, A.; Mueller, D. *J. Biol. Chem.* **2009**, *284*, 10546.
(38) Kutzner, C.; Czub, J.; Grubmüller, H. *J. Chem. Theory Comput.* **2011**, *7*, 1381−1393.
(39) Seeliger, D.; De Groot, B. *J. Comput. Chem.* **2008**, *30*, 1160−1166.
(40) Jorgensen, W. L.; Chandrasekhar, J.; Madura, J. D.; Impey, R. W.; Klein, M. L. *J. Chem. Phys.* **1983**, *79*, 926−935.
(41) Kaminski, G. A.; Friesner, R. A.; Tirado-Rives, J.; Jorgensen, W. L. *J. Phys. Chem. B* **2001**, *105*, 6474−6487.
(42) Hess, B.; Kutzner, C.; van der Spoel, D.; Lindahl, E. *J. Chem. Theory Comput.* **2008**, *4*, 435−447.
(43) Nosé, S. *J. Chem. Phys.* **1984**, *81*, 511.
(44) Parinello, M.; Rahman, A. *J. Appl. Phys.* **1981**, *52*, 7182−7190.
(45) Essmann, U.; Perera, L.; Berkowitz, M. L.; Darden, T.; Lee, H.; Pedersen, L. G. *J. Chem. Phys.* **1995**, *103*, 8577−8593.
(46) Hess, B. *J. Chem. Theory Comput.* **2008**, *4*, 116−122.
(47) Miyamoto, S.; Kollman, P. A. *J. Comput. Chem.* **1992**, *13*, 952−962.
(48) Torrie, G. M.; Valleau, J. P. *J. Comput. Phys.* **1977**, *23*, 187−199.
(49) Kumar, S.; Bouzida, D.; Swendsen, R. H.; Kollman, P. A.; Rosenberg, J. M. *J. Comput. Chem.* **1992**, *13*, 1011−1021.
(50) Kabsch, W.; Sander, C. *Biopolymers* **1983**, *22*, 2577−2637.
(51) Humphrey, W.; Dalke, A.; Schulten, K. *J. Mol. Graph* **1996**, *14*, 33−38.
(52) Böckmann, R. A.; Grubmüller, H. *Nat. Struct. Biol.* **2002**, *9*, 198−202.
(53) Czub, J.; Grubmüller, H. *Proc. Natl. Acad. Sci. U. S. A.* **2011**, *108*, 7408−7413.
(54) Menz, R.; Walker, J.; Leslie, A. *Cell* **2001**, *106*, 331−341.
(55) Pänke, O.; Rumberg, B. *Biochim. Biophys. Acta* **1999**, *1412*, 118−128.
(56) Bock, L. V.; Blau, C.; Schröder, G. F.; Davydov, I. I.; Fischer, N.; Stark, H.; Rodnina, M. V.; Vaiana, A. C.; Grubmüller, H. *Nat. Struct. Mol. Biol.* **2013**, *20*, 1390−1396.
(57) Yoshidome, T.; Ito, Y.; Matubayasi, N.; Ikeguchi, M.; Kinoshita, M. *J. Chem. Phys.* **2012**, *137*, 035102.
(58) Ito, Y.; Yoshidome, T.; Matubayasi, N.; Kinoshita, M.; Ikeguchi, M. *J. Phys. Chem. B* **2013**, *117*, 3298−3307.